

Analysis of the domain interactions between the protease and helicase of NS3 in dengue and hepatitis C virus

L. Rosales-León, G. Ortega-Lule, B. Ruiz-Ordaz*

*Departamento de Biología Molecular y Biotecnología, Instituto de Investigaciones Biomédicas,
Universidad Nacional Autónoma de México, Ciudad Universitaria, Apartado Postal 70228, 04510 México, D.F., México*

Received 3 July 2005; received in revised form 1 April 2006; accepted 1 April 2006

Available online 11 May 2006

Abstract

Flaviviridae non-structural 3 protein (NS3) is a multifunctional enzyme, composed by a protease domain (NS3pro) and an RNA helicase domain (NS3hel). The activities present in NS3 have proved to be critical for viral replication. The replicative cycle of *Flaviviridae* requires coordinated regulation of all the activities present in the full-length NS3 protein, however, the exact nature of these interactions remains unclear. The present work aimed to determine common structural features between NS3 of dengue and hepatitis C viruses and to characterize residues involved in the regulation of the interdomain motions between NS3pro and NS3hel. Analysis of the root mean square (RMS) variation shows that NS3pro increases the stability of subdomain 1 of the RNA helicase. Moreover, the dynamic behaviour of the carboxy terminus of NS3hel, supports the hypothesis that, upon release of the carboxy-terminus from NS3pro, the residues involved in this interaction are folded back into the last α -helix. Using normal mode analysis, we characterized slow collective motions of NS3, and observed that the two lowest-frequency normal modes are enough to describe reorientations of NS3pro relative to NS3hel. These movements induced an increment in the exposure of the active site of NS3pro that can be important during the proteolytic processing of the viral polyprotein. The third low-frequency normal mode was correlated to subdomain reorientations of NS3hel, similar to those proposed during NTP hydrolysis and dsRNA unwinding. Based on these data, we support a dynamic model, in which the domain movements between NS3pro and NS3hel result in the regulation of its activities.

© 2006 Elsevier Inc. All rights reserved.

Keywords: NS3; Hepatitis C virus; Dengue virus; Protease/helicase; Normal mode analysis

1. Introduction

The *Flavivirus* non-structural protein 3 (NS3) is a multifunctional protein involved in polyprotein processing and viral replication [1]. This protein is composed of two domains, a serine protease, located at the N-terminal domain (NS3pro) comprising one-third of its length, and a helicase/NTPase C-terminal domain (NS3hel). Both domains and their activities have proved to be critical for viral replication in diverse members of the family [2,3]. NS3pro is responsible for the proteolytic cleavage of the viral polyprotein at the NS3/NS4a, NS4a/NS4b, NS4b/NS5a, and NS5a/NS5b junctions in the genus *Hepacivirus* [4–6] and at the virC/anchC, NS2a/NS2b, NS2b/NS3, NS3/NS4a, NS4a/NS4b and NS4b/NS5 in the genus *Flavivirus* [7,8]. It has also been shown that the activity

of the NS3 protease in both genera is enhanced by the association of an essential cofactor required for polyprotein maturation [9,10] (NS4a in *Hepacivirus* and NS2b in *Flavivirus*). In both genera, the cofactor is thought to associate to NS3pro by a central β -strand, effectively becoming an integral part of the β -barrel fold. Comparison of the different structures of the NS3pro from hepatitis C virus (HCV), both alone and in complex with a NS4a-derived peptide [11] suggested that the mechanism of cofactor-dependent catalysis enhancement is mediated by the local rearrangements of the catalytic triad towards a more catalytically favorable conformation. Recent molecular modelling studies in dengue virus (DENV) have shown that this mechanism is also feasible in *Flavivirus* [12].

NS3hel is responsible for unwinding the RNA duplexes occurring during viral replication. Despite the conservation of several sequence motifs in both domains, there are several differences between NS3 from different genera in the family, including the presence of an additional RNA 5'-triphosphatase

* Corresponding author. Tel.: +52 56 22 38 73; fax: +52 56 22 38 55.

E-mail address: bhro@servidor.unam.mx (B. Ruiz-Ordaz).

(RTPase) activity that is found exclusively in the NS3hel domain of the genus *Flavivirus* [13], as well as differences in NS3pro mechanisms of activation [14], specificity, and associated cofactors.

In 1999, Yao et al. [15] determined the structure of a single chain construct in which 13 residues of the NS4a cofactor precede the N-terminus of NS3 (scNS3-NS4a). In this structure, NS3pro exhibits the dual β -barrel fold, typical of the chymotrypsin-related serine proteases. NS3hel is composed by two structurally related β - α - β subdomains, homologous to other helicases and a third α -helical subdomain, unique to the flaviviral helicases. One of the most striking features of the structure is the arrangement of both domains, connected by a long extended chain with the active site of the NS3 proteinase oriented towards the interface between NS3pro and NS3hel. As there is no evidence of proteolytic processing of NS3 in vivo, local and global conformational changes are needed during the cleavage of the NS3–NS4a scissile bond (an intramolecular proteolysis event, also termed a *cis* cleavage) as well as during the subsequent NS3-mediated processing of the polyprotein precursor (termed *trans* cleavages, as they are involved in the recognition of polyprotein cleavage junctions by an NS3 molecule of another polypeptide) [15].

In spite of data from several groups that point to the importance of the interdomain interactions between NS3pro and NS3hel in the regulation of their activities, the extent and nature of these interactions are not clear yet. Morgenstern et al. reported that the addition of poly(U) causes a five-fold stimulation of the protease activity of the NS3–NS4a complex of HCV isolated from transfected COS cells [16], pointing towards a possible interdependency between the RNA helicase and serine protease activities. In contrast, Gallinari et al. [17] working with full-length NS3 associated to a synthetic NS4a peptide, found protease activity inhibited as a result of the addition of poly(U)/oligo(U)₁₈. As the protease domain alone showed similar inhibition levels, RNA-mediated inhibition was proposed to be caused by direct interaction with NS3pro.

A recent study by Drouet et al. demonstrated the interaction between some inhibitors of the serpin family and NS3, however, only the complete polypeptide can produce high molecular weight reaction products [18]. Similarly, Johansson et al. found an important effect of the presence of the helicase on the product-based inhibition of the serine protease. Interestingly, they observed that shortened products retain better inhibitory potency in the full-length polypeptide, compared to the minimal protease domain [19]. In a similar way, Gallinari shows that ATPase activity of full-length NS3 shows greater stimulation in response to the addition of poly(U) compared to ATPase activity stimulation observed on the helicase domain alone [17]. The replicative cycle of flaviviridae requires coordinated regulation of all the activities present in full-length NS3. However, given its unique domain arrangement, the exact nature of these interactions remains unclear, and further functional and structural data are needed in order to gain a deeper understanding of this multifunctional protein. The present work aims to determine common structural features between NS3 of dengue virus (DENV) and hepatitis C virus

(HCV), and to characterize the residues involved in the regulation of the interdomain motions between NS3pro and NS3hel.

2. Methods

2.1. Construction of the DENV NS3 model

The 3D coordinates of the NS3 protein of DENV NS3 (1BEF) protease and helicase (2BHR) domains were extracted from the Protein Data Bank, PDB [20]. The atomic structures were generated using MODELLER [21], based on the structural alignment with the homologous HCV structure reported by Yao et al. (1CU1). The refinement of the resulting NS3-DENV polypeptide was adopted from Selisko et al. [22] and carried out by the X-PLOR [23] program in several steps: initially the model was subjected to energy minimization using the Powell minimizer (minimization parameters: 200 steps, initial drop in energy 40.0 kcal mol⁻¹, harmonic energy constant 40.0 kcal mol⁻¹ Å⁻²) and restrained molecular dynamics (all α atoms fixed, time step 0.5 fs, 200 steps, initial temperature 300 K). The next refinement step consisted of 50 cycles alternating a rigid body minimization process (50 steps, initial drop in energy of 0.1 kcal mol⁻¹, rigid entities were the protease domain, the interdomain chain and the RNA helicase domain) with a molecular dynamics process (all α atoms fixed, time step 0.2 fs, 200 steps, initial temperature 300 °K). Finally, the model was further refined using the NAMD2 molecular dynamics program [24] with the CHARMM27 potential set [25,26]. The system setup included the particle mesh Ewald (PME) method for long range electrostatics [27], a 10 Å cut-off for van der Waals interactions and periodic boundary conditions allowing a minimum distance of 5 Å from the model to the boundary of the box. All bonds involving hydrogen atoms were constrained using the SHAKE algorithm [28] to allow a timestep of 2 fs.

To generate the solvent, a box of dimensions 96.0 Å × 93.0 Å × 98.5 Å was filled with molecules of water and overlapping waters were removed using the program Visual Molecular Dynamics (VMD) [29]. The refinement protocol consisted in: [1] energy minimization, 2500 steps, [2] 2 cycles of molecular dynamics (MD) (100 fs) and energy minimization (1000 steps), backbone atoms fixed, [3] 2 cycles of MD (100 fs) and energy minimization (1000 steps) C α atoms restrained, [4] 2 cycles of unrestrained MD (100 fs) and energy minimization (1000 steps), [5] energy minimization, 2500 steps. To study the overall stability of the model, the solvent/protein system was equilibrated at 298 K for 1 ns of MD and the trajectory of the simulation was sampled every 10 ps.

2.2. Molecular dynamics of NS3

To evaluate the differences in the stability and dynamic behaviour of NS3/4a and NS3hel (residues 201–631) for HCV, MD were performed on models of both polypeptides. Atomic coordinates for NS3hel were obtained from an edited version of the 1CU1 structure, removing residues 705–720 (NS4a peptide)

and 3–200 (NS3pro plus the interdomain chain). Simulations for all models were performed in NAMD2, with the CHARMM27 potential set under the same system setup conditions as above. Initially, an assembly was generated consisting of the NS3/4a fusion protein immersed in a box of TIP3 water molecules of dimensions $74 \text{ \AA} \times 79 \text{ \AA} \times 89 \text{ \AA}$. The simulation protocol consisted of 1000 steps of energy minimization of the protein/solvent system, and molecular dynamics of the protein/solvent system for 1 ns at 300 K, sampling the trajectory every 2 ps. An identical protocol was employed for NS3hel coordinates adjusting the boundary conditions to a box of $74 \text{ \AA} \times 79 \text{ \AA} \times 61 \text{ \AA}$.

Overall structure variations were analyzed by aligning the sampled conformations for both trajectories and calculating the root mean square deviation (RMSD) of the C α with VMD. To obtain a better insight of the differences in dynamic behaviour between NS3/4a and NS3hel, each trajectory was aligned considering only the C α of the helicase domain and RMSD variations for each residue were calculated along the 1 ns time space, using VMD.

2.3. Normal mode analysis

Normal mode analysis (NMA) of NS3 from HCV and DENV was performed with the help of ElNemo [30], a web interface to the Elastic Network Model. Briefly, the NMA calculations are based on the harmonic approximation of the potential energy around a minimum energy conformation. ElNemo takes advantage of the original implementation from Tirion [31], where detailed, empirical forcefields are replaced by a single parameter Hookean potential, avoiding the need for long energy minimizations previous to NMA calculations. Another advantage of the ElNemo approach is

the use of rotation-translation blocks (RTB), allowing the treatment of models at with atomic detail, while reducing the computation times. The use of this approximation has been shown to have little impact on the low frequency normal modes. For the present work, we used a distance cutoff of 9 Å and an RTB size of one, as these parameters gave the best correlation values between the computed and the observed B factors. The amplitude of the perturbation applied to every normal mode was based on the conservation of the secondary structure and the presence of steric clashes, evaluated with PROCHECK [32]. The relative movement associated to each normal mode was analyzed with the DynDom 1.5 [33] package.

2.4. Interactive dynamics simulations

Interactive simulations of NS3-HCV used the structure reported by Yao et al. As described previously, the fully solvated system was equilibrated for 1 ns. To simulate the system at the speed necessary for interaction, several simplifications were required. Only water molecules and residues in a radius of 6 Å around the COOH terminus were included in the simulation. The number of water molecules included in the system ensured the availability of enough water to replace the COOH terminus along its movement. The simplified system contained 4617 atoms, 1950 of which were free to move. The interactive simulations used the CHARMM27 force field. The system was maintained at a temperature of 310 K through Langevin damping with a coefficient of 10 ps^{-1} , and the nonbonded interactions were simulated with a 10 Å cutoff. Four interactive simulations were performed. The COOH terminus was pulled slowly through the interface between the protease and the helicase, over 1 h of real

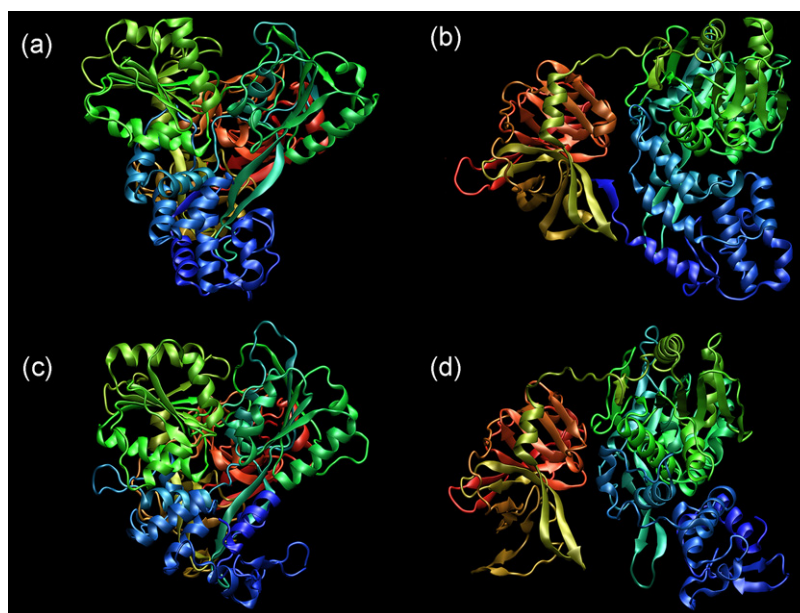


Fig. 1. Structure of NS3 proteins from Flaviviridae. (a) Cartoon representation of scNS3–NS4a from HCV, view from the helicase domain, (b) scNS3–NS4a, lateral view, the protein has been rotated 90° counterclockwise over the y-axis with respect to the view from (a). (c) Cartoon representation of the scNS3–NS2a model from DENV, the orientation of the protein is similar as (a), (d) scNS3–NS2b, lateral view, the protein has been rotated 90° counterclockwise over the y-axis with respect to the view from (c).

time (~100 ps of simulated time). All interactive simulations were run on a SGI Onix using 10 R14000 processors.

3. Results and discussion

3.1. Dengue NS3 model

We were able to generate a model for the DENV-NS3 protein based on the reported structure for the full length polypeptide of HCV. Overall, our model shows a different interface compared to the reference molecule, 1CU1, due to the different structure on the third helicase subdomain between HCV and DENV (Fig. 1). The adopted refinement strategy allowed interface optimization by side chain readjustment and optimization of the relative orientation between the functional domains of DENV-NS3. The whole NS3 model is composed of 635 residues organized in five sub-domains. The interdomain chain has a random coil conformation with the contact regions involving the amino and carboxy region of the protease and the second sub-domain of the viral helicase. The interface between both domains is composed with 12 residues of the serine protease and 15 residues of the RNA helicase. The local interactions on the interface are mainly hydrophobic, with the presence of six hydrogen bonds with residues from the adjacent domains.

We evaluated the stability of the model over a long MD simulation. The RMSD variation in Fig. 2a shows that after 100 ps, a plateau was reached, indicating that equilibrium was achieved during the simulation. The overall RMSD for the 500 sampled conformations along the trajectory is 1.49 Å, with the

higher mobility regions associated to residues present in loops, indicating the stability of the secondary structure (Fig. 2b).

3.2. Molecular dynamics simulation of scNS3-NS4a and NS3hel

A 1 ns, 300 K MD simulation was carried out for the solvated 1CU1 structure, in the absence of a bound ligand. The main objective was to compare the dynamic behaviour of the entire NS3 polypeptide to that of the helicase domain, to find mobility differences caused by the interaction between the protease and the helicase domains. To achieve this, we sampled 500 conformations along the MD simulation and calculated their RMSD. Fig. 3a presents a plot of the RMSD for the C α traces of the NS3 and NS3hel structures along the simulation, (both trajectories compared against the initial $T=0$ ns structure). The RMSD of NS3 reaches a plateau just after 100 ps, indicating that the system is equilibrated, however, the structure of NS3hel takes longer to reach a stable set of conformations. These differences can be attributed to the stabilizing effect of the protease domain on the residues involved in the interface with the helicase domain, mainly at the carboxy terminus, which is in direct contact with the protease active site. To determine with more detail the residues involved in the mobility differences, we calculated the RMSD of the α carbons of the helicase domain for both trajectories. Finally, we compared these average RMS deviations between equivalent residues of NS3/4a against NS3hel. Fig. 3b shows the normalized RMSD along the protein sequence. We observed

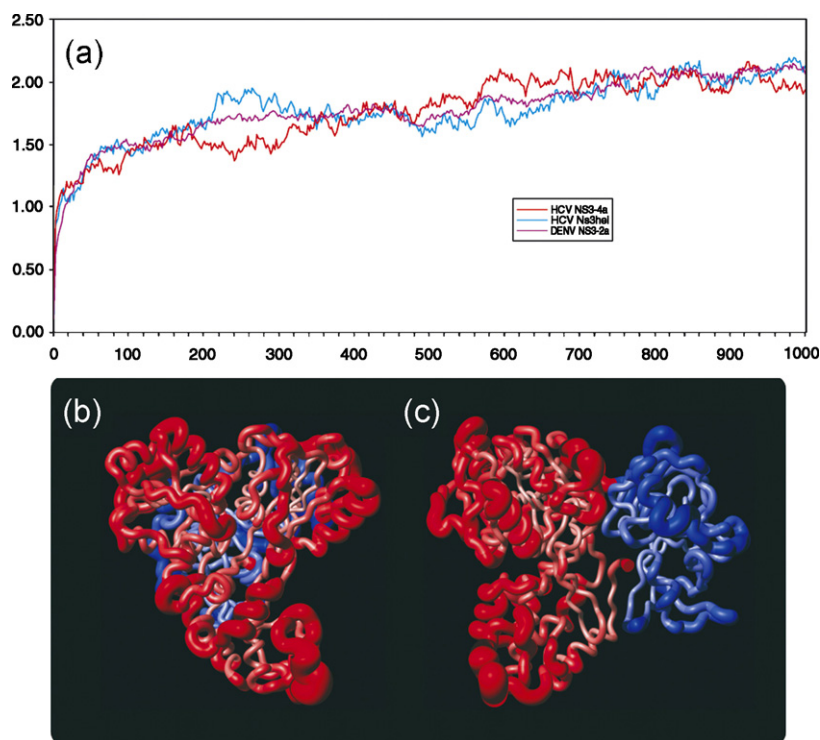


Fig. 2. Analysis of the dynamic behaviour of DENV NS3 on MD simulations. (a) RMSD of the C α for HCV NS3–NS4a (red), HCV NS3hel (blue line) and DENV ScNS3–NS2a (purple line) over a 1 ns simulation. Measured structure variations are relative to the initial ($T=0$) structure. (b) Ribbon representation of the ScNS3–NS2a model from DENV. The width of the ribbon and the color intensity represent the RMSD value over the C α trace. NS3pro and NS3hel are shown in blue and red, respectively (c) 90° rotation over the y-axis of the ribbon representation shown in (b).

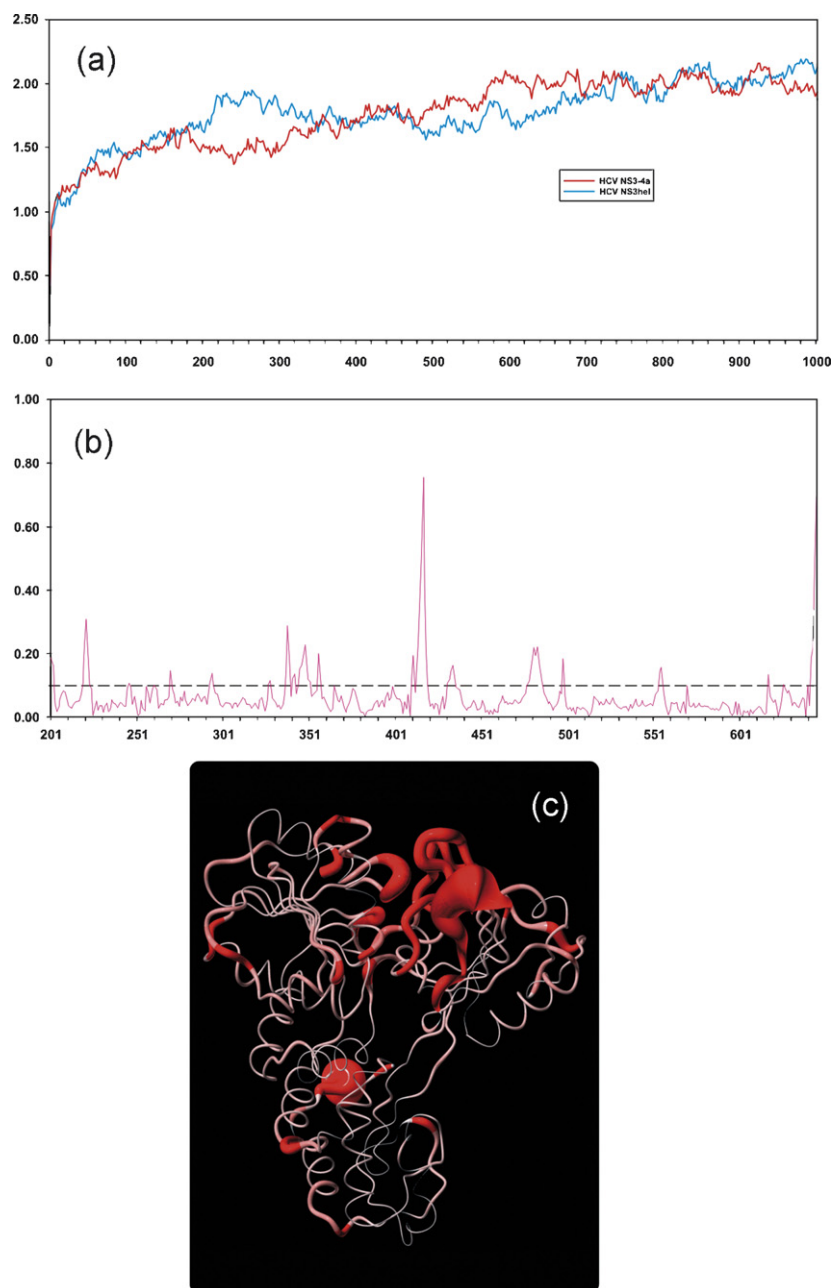


Fig. 3. Analysis of the dynamic behaviour of HCV NS3 on MD simulations. (a) RMSD of the C α for HCV NS3–NS4a (red) and HCV NS3hel over a 1 ns simulation. Measured structure variations are relative to the initial ($T = 0$) structure. (b) Differences in the mobility per residue between NS3–NS4a and NS3hel. Each point represents the difference, expressed as absolute values, between the RMSD obtained for the isolated helicase domain and for NS3–NS4a. The broken line represents the standard deviation of all the measured differences. (c) Ribbon representation of the helicase domain of NS3 from HCV. The width of the ribbon represents the relative differences in RMSD between the isolated helicase domain and NS3–NS4a. Residues highlighted in red have differences greater than 1 standard deviation.

that almost 90% of the residues have normalized differences below 0.19, however, the overall distribution of the remaining 10% is not evenly distributed along the helicase domain. In Fig. 3c, all the residues with RMS differences above 0.19 are mapped on the mean structure of the 1CU1 protein (the radius of the ribbon representing the RMS deviations from the C α trace). As shown, almost all of these residues fall in two loops located between subdomains 2 and 3 of NS3hel. Note that the ribbon trace has a very small radius at most parts of the protein, showing the overall stability of the secondary structure. Together, these data suggest that the presence of the serin

protease domain exerts an important effect that increases the stability of the subdomain 1 of the RNA helicase, which includes many of the residues involved in the binding and hydrolysis of NTPs.

In addition, the MD simulation of the NS3hel coordinates provides important structural information about the behaviour in solution of the carboxy terminus of the helicase domain. From the trajectory data analyzed it is possible to observe that the length of the last α -helix increases as the simulation progresses (Supp Material 1). These changes were proposed by Yao et al. on the basis of a comparison between their data and

Table 1
Analysis of the dynamic domains of the three lowest-frequency normal modes of HCV-NS3

Normal mode	Fixed domain ^a (RMSD)	Moving domain ^b (RMSD)	Connecting regions	Angle of rotation (°)	% of closure motion	Angle ^c (°)
Mode 7	Domain 1 (297 residues) [0.642 Å] Domain 2 (193 residues) [0.796 Å]	Domain 2 (193 residues) [0.796 Å]	181–188	30.6	4.44	12.0
			431–435	15.7	5.99	14.0
			446–451 480–487 509–520 523–525			
		Domain 3 (151 residues) [0.754 Å]	157–165 622–629	33.8	83.30	65.0
Mode 8	Domain 1 (200 residues) [0.836 Å]	Domain 2 (265 residues) [0.748 Å]	184–193	35.6	96.2	78.7
			622–628 202–205 321–322 327–333	31.0	66.5	54.6
			433–434 448–449 453–458 477–487	33.8	83.30	65
		Domain 3 (173 residues) [0.521 Å]				
Mode 9	Domain 1 (408 residues) [0.964 Å]	Domain 2 (131 residues) [0.475 Å]	324–329 429–435 448–458 477–499	16.9°	73.3	58.9
			432–436 445–446 527–532 623–625	18.0°	99.1	84.5
		Domain 3 (102 residues) [0.715 Å]				

^a Domain is defined as a quasi-rigid body cluster of residues with different rotational properties from the rest of the polypeptide.

^b Moving domain determined relative to the fixed domain.

^c Defined as the angle between the screw axis and a line joining the centers of mass from the moving and fixed domains.

previously reported structures for the isolated helicase domain. However, all structures reported to date for the NS3hel have missing carboxy terminal residues, due to the high mobility of this region. Our data support the hypothesis that upon release of the carboxy terminus from NS3pro, part of the residues involved in this interaction are folded back into the last α -helix. However, the last five residues remain in an extended state; allowing them to form again the interface with NS3pro. In agreement with this, in a recent study, Wang et al. proposed that the conservation of the invariable residue Thr instead of the optimal residue Cys at the carboxy terminus of NS3 (corresponding to the P1 site of the NS3–NS4a cleavage site) is needed to prevent subsequent product inhibition of NS3pro in the full-length polypeptide [34].

3.2.1. Normal mode analysis in HCV NS3

In order to analyze the dynamic properties of full-length NS3, we carried out an NMA of the HCV model. The use of ElNemo allowed us to analyze the all-atoms models, with one residue at each RTB. Previous work from Tama et al. [35] has shown that the use of this approximation has little impact on the calculated modes. Of the NMA of NS3, we will here discuss the three lowest frequency normal modes (modes 7–9, after the first

six trivial modes have been discarded) and their possible functional significance. Table 1 shows the features of all domain motions associated to these modes.

Normal mode 7 describes a rotational movement of the protease relative to subdomains 1 and 2 of the helicase, involving a hinge region in the residues 181–188 (purple ribbon, Fig. 4a, Supp Material 2), the screw axis is almost perpendicular to the interface between both regions. This movement is coupled to a 15.7° rotation of subdomain 3 of the helicase, relative to subdomains 1 and 2 and involves 5 bending segments (residues 431–435, 446–451, 480–487, 509–520, 523–525; Fig. 4b, green ribbon) with a screw axis perpendicular to the first one. The interface between the protease and the subdomain 3 of the HCV helicase is not disrupted for the chosen amplitudes, however, most of the interface is involved in the flexible regions that couple movement between both domains.

Normal mode 8 is a closure movement between the protease and the helicase (Fig. 4c and d & Supp Material 3), again, subdomains 1 and 2 of the helicase form a quasi-rigid unit, in this normal mode the screw axis associated to the opening/closure of the protease is almost parallel to its interface with the helicase. Moreover, the movement of the protease is coupled to

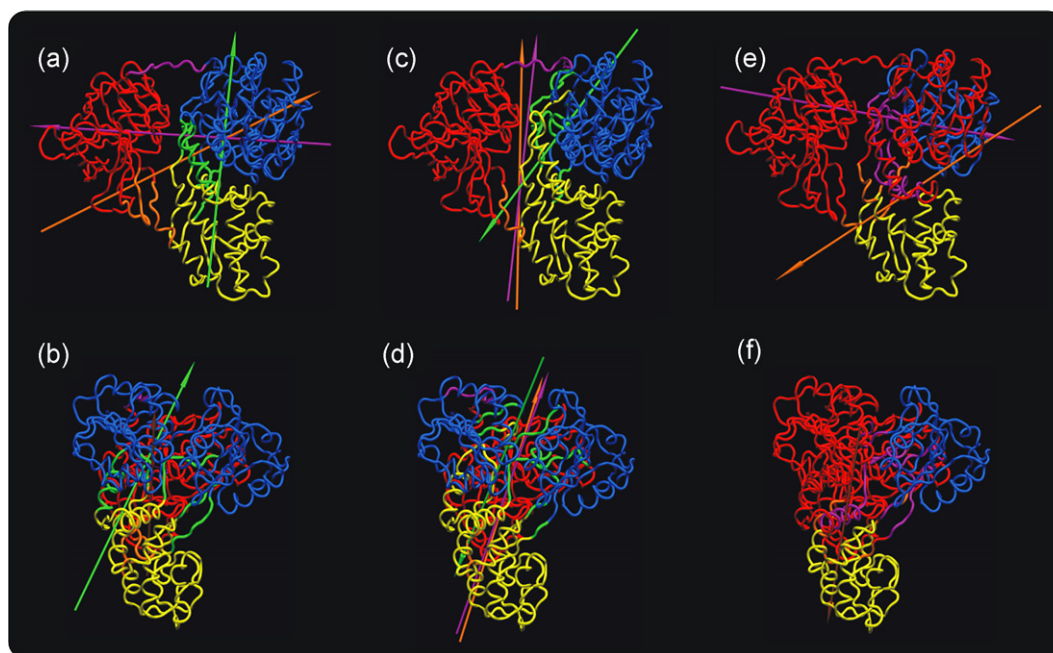


Fig. 4. Dynamic domains associated with the three lowest-frequency Normal Modes for scNS3-NS4a. Dynamic domains are shown in red, blue and yellow ribbons, while the flexible regions are represented as purple (bending residues between red and blue domains), orange (bending residues between red and yellow domains) and green (bending residues between blue and yellow domains) ribbons. Screw axes are represented as arrows with the same color scheme as the flexible regions. (a) Normal mode 7, frontal view of NS3hel. (b) Normal mode 7, 90° rotation over the y-axis of the view in (a). (c) Normal mode 8, frontal view of NS3hel. (d) Normal mode 7, 90° rotation over the y-axis of the view in (c). (e) Normal mode 8, frontal view of NS3hel. (f) Normal mode 9, 90° rotation over the y-axis of the view in (e).

a reorientation of the subdomain 3 of NS3hel, however, this movement is more limited than the reorientation present in mode 7. Again, the interface between the protease and the subdomain 3 of the helicase is not disrupted for the chosen amplitudes, and most of the hinge residues belong to this region.

According to our data, the protease movements described in the normal modes 7 and 8 are coupled to the helicase by the residues at the interface between them, in particular, we found three regions (56, 78, 79), (326–327 524) and (483–485 520–522) that lie in close proximity to the screw axis in both modes that could act as pivot points. Moreover, residues 613–623 (α -helix) and 430–452 (beta hairpin) are of great importance as mechanical hinges, coupling the movements of the protease domain to the helicase subdomain 3.

Normal mode 9 describes a closure movement between the subdomains 2 and 3 of NS3hel, while the protease domain in conjunction with the first subdomain of NS3hel behaves as a quasi-rigid unit (red ribbon, Fig. 4e and f, Supp Material 4). In this mode, there are several residues acting as a hinge for the displacement of subdomain 1 (454–457, 480–483) as well as subdomain 2 (532, 623–624).

3.2.2. Normal mode analysis in DENV NS3

Next, we analyzed the dynamic behaviour of the DENV NS3 full-length model, in order to compare the dynamic properties of this model with those of the HCV full-length NS3. Table 2 shows the features of all domain motions associated to the normal modes analyzed. Not surprisingly, DENV NS3 shows a greater number of low frequency modes associated to high

collectivity values. As the proposed model for this protein lacks the contacts present in the carboxy terminus of the HCV NS3 model, it is expected that a greater number of high collectivity movements will be present, since the protease domain will have more degrees of freedom to move. According to our analysis with DynDom, the first five low frequency normal modes have domain motions that are roughly equivalent to modes 7, 8 and 9 of the HCV NS3.

3.3. Interactive dynamics simulations

IMD was used to characterize the possible mechanisms that regulate the exposure of the protease active site of HCV NS3 protein. The IMD simulations began with the COOH terminus of the model positioned over the active site of the protease domain. However, as seen in the non-interactive simulations, thermal motion was not enough to free the atoms of the COOH terminus from the protease active site. In order to accelerate this process, a force was applied to this zone. Our results show that, for the model derived from the experimental structure (1CU1), there are several steric impediments that keep the carboxy terminus in position and block water molecules from competing for hydrogen bonds in the interface. In order to test if the opening of the interface between the protease and the helicase was enough to allow the carboxy terminus to be released and interact with the solvent, we made further simulations starting with a conformation derived from the normal mode 8. The possibility that a reorientation of the domains present in NS3 was needed for the release of the COOH terminus and consequent exposure of the protease active site was first

Table 2
Analysis of the dynamic domains of the three lowest-frequency normal modes of DENV-NS3

Normal mode	Fixed domain ^a (RMSD)	Moving domain ^b (RMSD)	Connecting regions	Angle of rotation (°)	% of closure motion	Angle ^c (°)
Mode 7	Domain 1 (197 residues) [1.428 Å]	Domain 2 (434 residues) [0.831 Å]	194–204	30.0	44.73	41.9
Mode 8	Domain 4 (309 residues) [0.943 Å]	Domain 3 (103 residues) [0.619 Å]	187–204	29.5	8.7	17.1
		Domain 1 (89 residues) [0.713 Å]	335–341 491–500	26.2	81.5	64.5
		Domain 2 (117 residues) [0.782 Å]	445–451 459–463 507–513 532–534	13.6	62.24	52.0
		Domain 1 (89 residues) [0.713 Å]	42–44 55–56 64–65 97–98	9.7	99.4	85.7
Mode 9	Domain 2 (114 residues) [1.359 Å]	Domain 3 (84 residues) [0.848 Å]	101–103 184–187	15.8	12.2	20.5
		Domain 1 (433 residues) [1.473 Å]	191–204 338–340 494–499	24.8	95.8	77.7
Mode 10	Domain 3 (328 residues) [2.000 Å]	Domain 1 (189 residues) [0.878 Å]	185–203 338–340	24.4	88.2	69.9
		Domain 2 (100 residues) [1.743 Å]	446–455 458–462 541–547	37.2	35.3	36.4
Mode 11	Domain 2 (352 residues) [2.754 Å]	Domain 2 (178 residues) [1.428 Å]	205–208 212–225 240–247 301–302 305–306 331–332 446–447 460–463 502–503	19.7	92.8	74.5
		Domain 3 (101 residues) [1.573 Å]	449–450 459–461 542–544	22.4	99.4	85.6

^a Domain is defined as a quasi-rigid body cluster of residues with different rotational properties from the rest of the polypeptide.

^b Moving domain determined relative to the fixed domain.

^c Defined as the angle between the screw axis and a line joining the centers of mass from the moving and fixed domains.

proposed by Yao et al. Our IMD simulations support this hypothesis, indicating that an opening motion similar to those observed in the normal modes 7 and 8 can be necessary to allow water to reach the protease active site. Once water molecules have reached the active site, they can facilitate the unbinding of the carboxy terminus by competing with it for hydrogen bond formation.

4. Conclusion

To complement the structural data and molecular dynamics simulations of NS3, we performed normal mode calculations with an all-atoms model that explicitly includes the individual atomic interactions. Our analysis predicts the presence of hinge residues between NS3pro and NS3hel. These flexible regions

are associated to at least two types of motions: a twisting movement and an opening/closure movement. The changes associated to these movements include the coupling of the reorientation of the protease domain to a limited rotation of the helicase subdomain 3. An additional pivot point is composed of the residues of the interdomain chain. The normal mode calculations reported here reveal important features of the flexibility of the segments involved at the interface between NS3hel and NS3pro. As proposed previously for the F₁-ATPase, both domains have encoded the structural plasticity that is essential for their function [36]. In particular, the third subdomain of the NS3 shows the intrinsic flexibility to couple movements between NS3pro and NS3hel. In agreement with the previous work of Yao et al. we support the hypothesis that NS3 is able to regulate the activities present in its domains by

modification of the interactions between the helicase and the serin protease domains (low frequency movements, associated to slow, large scale conformational movements), coupled to small rearrangements of the side chains on the hinge residues (higher frequency movements associated to the highly flexible regions) and changes in the electrostatic potential of the surface. It has been shown that the protease domain is able to contribute binding sites for RNA [7] in the full-length protein; thus, the position of this domain relative to the helicase RNA could play an important role in the regulation of the unwinding activity of the latter. In addition, it is highly plausible that the domain motions associated to normal modes 7 & 8 accounts for the necessary changes at the interface between both domains to increase exposure of the protease active site, making it more accessible to the substrate/solvent. Our IMD analysis shows that this domain reorientation is an important step in the release of the carboxy terminus from the protease active site of HCV NS3, by making the hydrogen bonds available to the solvent. Experimental results by Howe et al. [37], suggest that the presence of the protease domain associated to the core residues of NS4a enhances helicase activity. Likewise, Lam et al. [38], have shown that the presence of an intact protease domain enhances dsRNA unwinding when NS3hel is compared to full-length HCV NS3. Moreover, their data suggest that NS3pro promotes a more efficient usage of ATP hydrolysis during RNA unwinding. All of these results, together with the data from the MD simulations point towards a role of NS3pro in enhancing the RNA helicase/NTPase activities of NS3, perhaps by stabilizing and promoting a more active conformation of the residues associated with RNA binding/NTP hydrolysis.

Regarding DENV NS3, we have shown that the proposed association for the protease and the helicase domains is stable over a 1 ns simulation. At the writing of this manuscript, the biological significance of the proteolysis events for DENV NS3 that have been observed *in vitro* remain unclear, thus is highly possible that the protease domain participates in nucleic acid binding, as proposed previously by Xu et al. on the basis of molecular modeling [39]. One of the more notorious features of this model compared to the experimental structure of HCV (1CU1), is the lack of association between the carboxy terminus and the protease domain. As a result of this, the movements of the latter are associated to a greater number of low frequency normal modes. However, from our analysis, several common structural features can be derived; in particular, it is clear that the hinge regions present in subdomain 2 of the helicase can play an important role in the movements of this domain. Moreover, it is clear that movements of this subdomain are associated to limited reorientations of the third subdomain of the helicase in both models, pointing to a common structural mechanism that could be associated to the biological function of this family of enzymes.

Our analysis provides new insight into the biological significance of the structural rearrangements between the protease and helicase domains, and the role of these changes in the regulation of the activities of full-length polypeptides. In particular, the complex NS3pro-NS4a appears to play an important role in the uncoupling of the ATPase/ssRNA binding

and RNA unwinding activities [40,41]. Thus, the changes in relative protease orientation can be an important factor in the regulation of the NS4a effect on the helicase domain in members of the *Flaviviridae* family.

Acknowledgements

All the Interactive Molecular Dynamics simulations were done on the facilities of the Ixtli visualization observatory at the DGSCA, UNAM. The authors wish to thank the CONACyT, DGAPA, PAPPIT, DGSCA, and especially Dr. Luis Miguel de la Cruz Salas from the Visualization Laboratory of DGSCA for the support granted to the Ph.D. student Luis Rosales León.

We also wish to thank Ms. Isabel Pérez Montfort for English correction, Ms. Eva María Reyes for preparation of the manuscript and Dr. Veronica Monroy for technical assistance.

Appendix A. Supplementary data

Supplementary data associated with this article can be found, in the online version, at doi:10.1016/j.jmngm.2006.04.001.

References

- [1] V.V. Sardana, J.T. Blue, J. Zugay-Murphy, M.K. Sardana, L.C. Kuo, An uniquely purified HCV NS3 protease and NS4A21-34 peptide form a highly active serine protease complex in peptide hydrolysis, *Protein Expres. Purif.* 16 (1999) 440–447.
- [2] A.A. Kolykhalov, K. Mihalik, S.M. Feinstone, C.M. Rice, Hepatitis C virus-encoded enzymatic activities and conserved RNA elements in the 3' nontranslated region are essential for virus replication in vivo, *J. Virol.* 74 (2000) 2046–2051.
- [3] A.E. Matusan, M.J. Pryor, A.D. Davidson, P.J. Wright, Mutagenesis of the dengue virus type 2 NS3 protein within and outside helicase motifs: effects on enzyme activity and virus replication, *J. Virol.* 75 (2001) 9633–9643.
- [4] A. Grakoui, C. Wychowski, C. Lin, S.M. Feinstone, C.M. Rice, Expression, Identification of hepatitis C virus polypeptide cleavage products, *J. Virol.* 67 (1993) 1385–1395.
- [5] R. Bartenschlager, L. Ahlborn-Laake, J. Mous, H. Jacobsen, Nonstructural protein 3 of the hepatitis C virus encodes a serine-type proteinase required for cleavage at the NS3/4 and NS4/5 junctions, *J. Virol.* 67 (1993) 3835–3844.
- [6] A. Grakoui, D.W. McCourt, C. Wychowski, S.M. Feinstone, C.M. Rice, Characterization of the hepatitis C virus-encoded serine proteinase: determination of proteinase-dependent polypeptide cleavage sites, *J. Virol.* 67 (1993) 2832–2843.
- [7] Rice, C.M. *Flaviviridae: the viruses and their replication*. In: Fields Virology, Fields, B., Knipe, D., Howley, P. (Eds.), 3rd ed., Lippincott-Raven, Philadelphia, PA, vol. 2, 1996, 931–959.
- [8] C.E. Stocks, M. Lobigs, Signal peptidase cleavage at the *Flavivirus* C–prM junction: dependence on the viral NS2B-3 protease for efficient processing requires determinants in C, the signal peptide, and prM, *J. Virol.* 72 (1998) 2141–2149.
- [9] R. Bartenschlager, V. Lohmann, T. Wilkinson, J.O. Koch, Complex formation between the NS3 serine-type proteinase of the hepatitis C Virus and NS4A and its importance for polypeptide maturation, *J. Virol.* 69 (1995) 7519–7528.
- [10] B. Falgout, M. Pethel, Y.M. Zhang, C.J. Lai, Both nonstructural proteins NS2B and NS3 are required for the proteolytic processing of dengue virus nonstructural proteins, *J. Virol.* 65 (1991) 2467–2475.
- [11] Y. Yan, Y. Li, S. Munshi, V. Sardana, J.L. Cole, M. Sardana, C. Steinkuehler, L. Tomei, R. De Francesco, L.C. Kuo, Z. Chen, Complex of NS3 protease and NS4A peptide of BK strain hepatitis C virus: a 2,2 a

- resolution structure in a hexagonal crystal form, *Protein Sci.* 7 (1998) 837–847.
- [12] S. Chanprapaph, P. Saparpakorn, C. Sangma, P. Niyomrattanakit, S. Hannongbua, C. Angsuthanasombat, G. Katzenmeier, Competitive inhibition of the dengue virus NS3 serine protease by synthetic peptides representing polyprotein cleavage sites, *Biochem. Biophys. Res. Commun.* 330 (2005) 1237–1246.
- [13] G. Barthelma, R. Padmanabhan, Expression, purification, and characterization of the RNA 5'-triphosphatase activity of dengue virus type 2 nonstructural protein 3, *Virology* 299 (2002) 122–132.
- [14] P. Niyomrattanakit, P. Winoyanuwattikun, S. Chanprapaph, C. Angsuthanasombat, S. Panyim, G. Katzenmeier, Identification of residues in the dengue virus type 2 NS2B cofactor that are critical for NS3 protease activation, *J. Virol.* 78 (2004) 13708–13716.
- [15] N.P. Yao, S.S. Reichert, W.W. Taremi, Prosise, P.C. Weber, Molecular views of viral polyprotein processing revealed by the crystal structure of the hepatitis C virus bifunctional protease–helicase, *Structure Fold. Des.* 7 (1999) 1353–1363.
- [16] K.A. Morgenstern, J.A. Landro, K. Hsiao, C. Lin, Y. Gu, M.S. Su, J.A. Thomson, Polynucleotide modulation of the protease, nucleoside triphosphatase, and helicase activities of a hepatitis C virus NS3-NS4A complex isolated from transfected COS cells, *J. Virol.* 71 (1997) 3767–3775.
- [17] P. Gallinari, D. Brennan, C. Nardi, M. Brunetti, L. Tomei, C. Steinkühler, R. De Francesco, Multiple enzymatic activities associated with recombinant NS3 protein of hepatitis C virus, *J. Virol.* 72 (1998) 6758–6769.
- [18] C. Drouet, L. Bouillet, F. Csopaki, M.G. Colomb, Hepatitis C virus serine protease interacts with the serpin C1 inhibitor, *FEBS Lett.* 458 (1999) 415–418.
- [19] A. Johansson, I. Hubatsch, E. Akerblom, G. Lindeberg, S. Winiwarter, U.H. Danielson, A. Hallberg, Inhibition of hepatitis C virus NS3 protease activity by product-based peptides is dependent on helicase domain, *Bioorg. Med. Chem. Lett.* 11 (2001) 203–206.
- [20] H.M. Berman, J. Westbrook, Z. Feng, G. Gilliland, T.N. Bhat, H. Weissig, I.N. Shindyalov, P.E. Bourne, The protein data Bank, *Nucleic Acids Res.* 28 (2000) 235–242.
- [21] A. Sali, T.L. Blundell, Comparative protein modelling by satisfaction of spatial restraints, *J. Mol. Biol.* 234 (1993) 779–815.
- [22] B. Selisko, A.F. Licea, B. Becerril, F. Zamudio, L.D. Possani, E. Horjales, Antibody BCF2 against scorpion toxin Cn2 from *Centruroides noxius* Hoffmann: primary structure and three-dimensional model as free Fv fragment and complexed with its antigen, *Proteins* 37 (1999) 130–143.
- [23] A.T. Brünger, J. Kuriyan, M. Karplus, Crystallographic R-factor refinement by molecular dynamics, *Science* 235 (1987) 458–460.
- [24] L. Kalé, R. Skeel, M. Bhandarkar, R. Brunner, A. Gursoy, N. Krawetz, J. Phillips, A. Shinozaki, K. Varadarajan, K. Schulten, NAMD2: Greater scalability for parallel molecular dynamics, *J. Comp. Phys.* 151 (1999) 283–312.
- [25] A.D. MacKerell Jr., D. Bashford, M. Bellott, R.L. Dunbrack Jr., J. Evanseck, M.J. Field, S. Fischer, J. Gao, H. Guo, S. Ha, D. Joseph, L. Kuchnir, K. Kuczera, F.T.K. Lau, C. Mattos, S. Michnick, T. Ngo, D.T. Nguyen, B. Prodhom, B. Roux, M. Schlenkrich, J. Smith, R. Stote, J. Straub, M. Watanabe, J. Wiorkiewicz-Kuczera, D. Yin, M. Karplus, Self-consistent parameterization of biomolecules for molecular modeling and condensed phase simulations, *FASEB J* 6 (1992) A143.
- [26] A.D. MacKerell Jr., D. Bashford, M. Bellott, R.L. Dunbrack Jr., J. Evanseck, M.J. Field, S. Fischer, J. Gao, H. Guo, S. Ha, D. Joseph, L. Kuchnir, K. Kuczera, F.T.K. Lau, C. Mattos, S. Michnick, T. Ngo, D.T. Nguyen, B. Prodhom, I.W.E. Reiher, B. Roux, M. Schlenkrich, J. Smith, R. Stote, J. Straub, M. Watanabe, J. Wiorkiewicz-Kuczera, D. Yin, M. Karplus, All-hydrogen empirical potential for molecular modeling and dynamics studies of proteins using the CHARMM22 force field, *J. Phys. Chem. B.* 102 (1998) 3586–3616.
- [27] T.A. Darden, D.M. York, L.G. Pedersen, Particle mesh Ewald. An N-log(N) method for Ewald sums in large systems, *J. Chem. Phys.* 98 (1993) 10089–10092.
- [28] J.P. Ryckaert, G. Ciccotti, H.J.C. Berendsen, Numerical integration of the cartesian equations of motion of a system with constraints: molecular dynamics of *n*-alkanes, *J. Comput. Phys.* 23 (1977) 327–341.
- [29] W. Humphrey, A. Dalke, K. Schulten, VMD – visual molecular dynamics. *J. Mol. Graphics* 14 (1996) 33–38 (<http://www.ks.uiuc.edu/Research/vmd/>).
- [30] S. Karsten, Y.H. Sanejouand, ElNémo: a normal mode web server for protein movement analysis and the generation of templates for molecular replacement, *Nucleic Acids Res.* 32 (2004) W610–W614.
- [31] M.M. Tirion, Large amplitude elastic motions in proteins from a single-parameter, atomic analysis, *Phys. Rev. Lett.* 77 (1996) 1905–1908.
- [32] R.A. Laskowski, M.W. MacArthur, D.S. Moss, J.M. Thornton, PROCHECK: a program to check the stereochemical quality of protein structures, *J. Appl. Crystallogr.* 26 (1993) 283–291.
- [33] S. Hayward, H.J.C. Berendsen, Systematic analysis of domain motions in proteins from conformational change: new results on citrate synthase and t4 lysozyme, *Proteins Structure Function and Genetics* 30 (1998) 144–154.
- [34] W. Wang, F.C. Lahser, M. Yi, J. Wright-Minogue, E. Xia, P.C. Weber, S.M. Lemon, B.A. Malcom, Conserved C-terminal threonine of hepatitis C virus NS3 regulates autoproteolysis and prevents product inhibition, *J. Virol.* 78 (2004) 700–709.
- [35] F. Tama, Y.H. Sanejouand, Conformational change of proteins arising from normal mode calculations, *Protein Eng.* 14 (2001) 1–6.
- [36] Q. Cui, G. Li, J. Ma, M. Karplus, A normal mode analysis of structural plasticity in the biomolecular motor F₁-ATPase, *J. Mol. Biol.* 340 (2004) 345–372.
- [37] A.Y. Howe, R. Chase, S.S. Taremi, C. Risano, B. Beyer, B. Malcolm, J.Y. Lau, A novel recombinant single-chain hepatitis C virus NS3-NS4A protein with improved helicase activity, *Protein Sci.* 8 (1999) 1332–1341.
- [38] A.M. Lam, R.S. Rypma, D.N. Frick, Enhanced nucleic acid binding to ATP-bound hepatitis C virus NS3 helicase at low pH activates RNA unwinding, *Nucleic Acids Res.* 32 (2004) 4060–4070.
- [39] T. Xu, A. Sampath, A. Chao, D. Wen, M. Nanao, P. Chene, S.G. Vasudevan, J. Lescar, Structure of the dengue virus helicase/nucleoside triphosphatase catalytic domain at a resolution of 2.4 Å, *J. Virol.* 79 (2005) 10278–10288.
- [40] P. Gallinari, C. Paolini, D. Brennan, C. Nardi, C. Steinkühler, R. De Francesco, Modulation of hepatitis C virus protease and helicase activities through the interaction with NS4a, *Biochemistry* 38 (1999) 5620–5632.
- [41] P.S. Pang, E. Jankowsky, P.J. Planet, A.M. Pyle, The hepatitis C viral NS3 protein is a processive DNA helicase with cofactor enhanced RNA unwinding, *EMBO J.* 21 (2002) 1168–1176.